Flood monitoring and mapping using passive microwave remote sensing in Namibia

Tom De Groeve [a]

[a] Joint Research Centre of the European Commission, Ispra, Via
Fermi 2147, 21020, Ispra, Italy

PLEASE SCROLL DOWN FOR ARTICLE

Taylor & Francis
Taylor & Francis Group

Flood monitoring and mapping using passive microwave remote sensing in Namibia

TOM DE GROEVE*

Joint Research Centre of the European Commission, Ispra, Via Fermi 2147, 21020 Ispra, Italy

Space-based river monitoring can provide a systematic, global, timely and impartial way to monitor disastrous floods. This paper describes a methodology to use daily passive microwave observations to detect, map and size floods, both for the purposes of global humanitarian organizations and national hydrological services. In the best case, floods can be detected as early as 2 h after they occur. Early warning is possible by monitoring upstream areas, with warning lead times up to 30 days. Flood maps are of a low resolution but match maps derived from high-resolution imagery. The interest lies in their daily availability, allowing us to understand the dynamic aspects of floods. Finally, objective flood sizing is achieved by integrating information over time and space. This paper details the results of the technique for the 2009 floods in Southern Africa and experiences for the 2010 flood season in Namibia.

1. Introduction

In 2008 and 2009, Namibia was affected by major floods, which caused more than 100 people to drown, affected more than 30% of the country's population and caused over US$200 million of losses (Van Langenhove 2009). In 2008 and 2009, very high rainfalls in the catchments of the Cuvelai, Kavango, Kwando and Zambezi rivers resulted in extreme floods (the worst in more than 40 years or longer). Because the frequency and magnitude of floods have been markedly reduced in the previous 25 years, they came as a total surprise. Conventional hydrological monitoring systems during floods, for both immediate and long-term purposes, are very vulnerable and have limited use for emergency response: the former because of ground inaccessibility and the latter because of lack of aerial information.

Although floods are the most frequent and recurring natural disasters (49%) consuming up to one-third of humanitarian aid (FTS OCHA, 2009), causing $20 billion annually in damages and affecting up to 100 million people annually (Rodriguez *et al. 20*09), there is no systematic, global and timely monitoring system available yet.

Floods are difficult to monitor on a global scale, because they are determined by local factors such as precipitation, slope of the terrain, drainage of the river, protection devices in place, etc. Each river must be monitored at different places

*Email: tom.de-groeve@jrc.ec.europa.eu

along its course. Although some flood disasters occur annually, most happen unexpectedly. About 2641 flood disasters were recorded in the Dartmouth Flood Observatory catalogue (DFO 2009), one of the most complete archives of flood events, between 2000 and 2007, affecting 2051 different rivers. Some rivers flooded more than 10 times (at different places along their course), but 1133 rivers flooded only once in 7 years. All rivers must therefore be monitored, and along their full course. The number of rivers in the world is hard to determine, but even the Digital Chart of the World (Danko 1992), a database at a scale of 1:1 million which shows only major rivers, has close to 1 million records, with a total length of 10 million km. Unlike for earthquakes where few measuring stations suffice to monitor the globe (the United States Geological survey global Seismographic network has less than 150 stations outside America), an in situ global flood monitoring system would need a dense network of gauging stations along all rivers. However, such stations are expensive (the United States Stream gauging Network costs US$89 million per year; USGS 1998), which makes this hardly feasible on a global scale.

On a global scale, humanitarian emergency responders do not have many information sources at their disposal to learn about flood disasters. Currently, they have to rely on media reports or their own global network of colleagues. One system providing a global list of flood events of potential humanitarian concern is the Global Disaster Alert and Coordination System (De Groeve 2007), but its data source is the media-based catalogue compiled manually at the Dartmouth Flood Observatory. Information is scattered and not standardized, making a global compilation and relative comparison of flood events difficult. Organizations that need to prioritize humanitarian aid between ongoing disasters need to do so on an ad hoc basis. As a consequence, aid is not always proportional to the size of the disaster (De Groeve and Riva 2009).

On a national scale, water authorities also face challenges to monitor their river network. First, the cost of maintaining gauging stations can be a limiting factor, in particular for large countries. While stations are out of service, there are gaps in the hydrograph time series. Second, rivers are often shared between countries, but information on floods in upstream countries is not always communicated to downstream countries. For adequate flood warning, countries need to be able to collect information over bordering countries independently. Third, gauging stations measure the water height, but not the extent of the flood. Obtaining information on the extent of the flood is a challenge for emergency managers, requiring aerial reconnaissance or satellite imagery.

In situ measurements can be replaced by remote sensing measurements, from airplanes or satellites. The change in surface water extent can be extracted from aerial or satellite imagery. While the use of sensors in the visible or infrared portion of the spectrum is limited due to cloud cover, the microwave portion of the spectrum can penetrate clouds (Smith 1997). However, for most remote sensing solutions, the revisit frequency (i.e. the time between two measurements in the same place) is too low for monitoring purposes, or the spatial coverage is limited (Bjerklie *et al.* 2003). For satellite based imagery, the revisit time depends on the orbit and the image size, and at least a few sensors have a daily revisit time and global coverage, and provide microwave data in near-real time free of charge. These are the Advanced Microwave Scanning Radiometer – Earth Observing System (AMSR-E) instrument on board of the NASA EOS Aqua satellite (launched in 2002) and the Tropical Rainfall Monitoring Mission (TRMM).

Using AMSR-E data, De Groeve *et al.* (2006) developed a method for detecting major floods on a global basis in a systematic, timely and impartial way appropriate for humanitarian response. Brakenridge *et al.* (2005) demonstrated that AMSR-E can measure river discharge changes in various climatic conditions. The methodology uses the brightness temperature at 36.5 GHz H-polarization during the descending (night) orbit of AMSR-E with a footprint size of approximately 8×12 km^2 and an average revisit time at 1 day. Brightness temperature is related to the physical temperature T and the emissivity ε of an object: $T_b = \varepsilon T$. Due to the different thermal inertia and emission properties of land and water, the observed microwave radiation in general accounts for a lower brightness temperature values for water ($T_{b,water}$) and higher for land ($T_{b,land} > T_{b,water}$). Since each observation of the satellite (or pixel) covers a relatively large area of 8×12 km^2, the observed brightness temperature is mostly composed of both water and land values, in proportion to the relative area of water (w) and land ($1 - w$) in the pixel.

$$T_b = (1 - w)T_{b,land} + wT_{b,water}, \tag{1}$$

where w is the water portion of the pixel.

If the physical temperature remains constant, changes in brightness temperature will be related to changes in water surface extent in the pixel. However, in spite of the great radiation dissimilarity of water and land cover, the raw brightness temperature observations cannot be used to reliably detect changes in surface water area. This is because brightness temperature (T_b) measures are influenced by other factors such as physical temperature, differences in emissivity and atmospheric moisture. While the relative contribution of these factors cannot be measured, they are assumed to be constant over a larger area. As shown in equation (2), the ratio between two nearby pixel values is a function of w alone. Therefore, by comparing a 'wet pixel' received over a river channel of a potential inundation location ($w > 0$) with a 'dry pixel' without water cover ($w = 0$), the mentioned noise factors can be reduced. The brightness temperature values of the measurement/wet signal are divided by the calibration/dry observations, referred to as M/C ratio or signal s.

$$
\begin{aligned}
T_{b,measurement} &= (1 - w)T_{b,land} + wT_{b,water} \\
&= T_{measurement}((1 - w)\varepsilon_{land} + w\varepsilon_{water}) \\
T_{b,calibration} &= T_{b,land} = T_{calibration}\varepsilon_{land}.
\end{aligned}
\tag{2}
$$

If, for nearby pixels, we assume

$$\varepsilon_{land,measurement} \approx \varepsilon_{land,calibration} \approx \varepsilon_{land}, T_{measurement} \approx T_{calibration} \tag{3}$$

then

$$
\begin{aligned}
s = \frac{M}{C} &= \frac{T_{b,measurement}}{T_{b,calibration}} = \frac{T_{measurement}((1 - w)\varepsilon_{land} + w\varepsilon_{water})}{T_{calibration}\varepsilon_{land}} \\
&\approx 1 - w + w\frac{\varepsilon_{water}}{\varepsilon_{land}} = f(w).
\end{aligned}
\tag{4}
$$

Typically, emissivity values for water are around 0.5, and for most minerals between 0.75 and 0.95 (Rees 1990). When calibration pixels are chosen carefully (without any open water), *s* varies between 1 ($w = 0$, no water) and 0.3 to 0.5 ($w = 1$, fully flooded) depending on the mineral content of the soil. In a time series, *s* is expected to vary with changes in water surface. Anomalies of the signal *s* can be correlated well with flood events. Moreover, as demonstrated by Brakenridge *et al.* (2007), if gauging data are available for the site, the signal can be calibrated to staging height with accurate results (figure 1).

De Groeve and Riva (2009) showed that a local maximum in a moving window (more specifically the local 95 percentile value in a window of 7×7 pixels) can be used for the calibration value, avoiding the need for manual selection of the calibration site. This finding extended the applicability of the method to any arbitrary area on Earth, rather than in carefully chosen sites, opening the way for a fully automatic global flood-detection system.

In order to distinguish between areas with permanent water (e.g. lakes or wide rivers) and areas with flood waters, one has to consider changes in flood signal over time. Based on a time series of 7 years (going back to June 2002 when the satellite was launched), anomalies are automatically detected using a method described by De Groeve *et al.* (2006). Since lower M/C signals generally account for increased water coverage, extreme events, or major floods, should represent negative anomalies in the time series of a given site. In order to detect anomalies, De Groeve *et al.* (2006) first determined the reference value for normal flow, which varies for each site based on the local emissivity properties and river geometry. This reference value was calculated as the average M/C value for the site since the launch of the satellite. They then set flood-level thresholds based on the statistics of the time series. Flood magnitude was defined as the number of standard deviations (SD) from the mean (avg):

$$m = \frac{s - \mathrm{avg}(s)}{\mathrm{SD}(s)}. \tag{5}$$

Floods appear typically for anomalies of 2 (small and regular flood) or 4 (large and unusual flood). This is equivalent to probabilities of 2.1% and 0.003%.
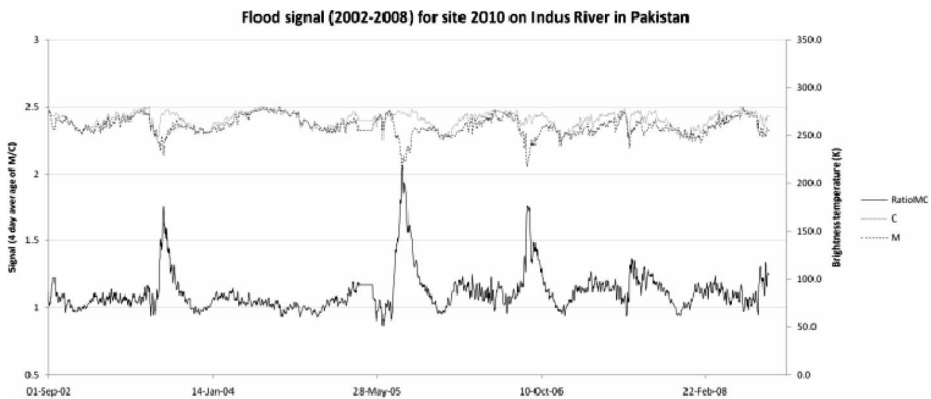

Figure 1.   Example of time series of $T_{\mathrm{b,measurement}}$ (*M*), $T_{\mathrm{b,calibration}}$ (*C*) and the flood signal *s* (RatioMC) for site 2010 100 km north of Hyderabad on the Indus River in Pakistan. The three peaks correspond to true flood disasters in 2003, 2005 and 2006.

The purpose of this paper is to demonstrate the usefulness and limitations of passive microwave satellite-based flood monitoring for humanitarian response and for national monitoring. While both communities have different requirements, they can both benefit from satellite-based flood monitoring technology, either as their sole source or as an additional, independent source to their toolset.

In particular, three aspects will be examined:

- Use for flood detection: can floods be reliably detected, and if so, is there a significant time gain compared with alternative methods?
- Use for real-time flood mapping: can water signal or magnitude images be used as flood maps, in order to visualise affected areas or the extent of the floods?
- Use for flood-size estimation: can floods of different years be compared in a quantitative way?

2. Methodology

In order to demonstrate the usefulness of passive microwave sensing for flood monitoring, an operational processing system was set up at the Joint Research Centre of the European Commission (JRC). In the development of this system, particular interest was focused on making the processing time as short as possible to approach real-time monitoring. Also, issues of reliability and redundancy were considered by using alternative sources of satellite data. This system has been in place since early 2009, but all data back to 2002 were reprocessed.

First, we describe the processing chain in detail. Subsequently, we describe the methodologies for addressing the three aspects: flood detection, flood mapping and flood sizing.

2.1 *Data processing*

The methodology has been tested with AMSR-E data and TRMM data. However, TRMM data are only available up to latitudes of 30°. In order to have global coverage, AMSR-E data are used.

The data used are the Level 1 brightness temperature at 36.5 GHz H-polarization during the descending (night) orbit of AMSR-E with a footprint size of approximately 8×12 km^2 and an average revisit time of 2 days south of 30° and 1 day north of 30° latitude. The swath data are available about 2 h after acquisition by the satellite from the Japanese Space Agency (Jaxa). About 24 h later, they are also available from the National Snow and Ice Data Centre (NSIDC) in the USA, which is used as a backup data provider.

The data are downloaded at JRC, resampled (using a nearest neighbour approach) and mosaicked in daily grids with global coverage; see De Groeve and Riva (2009) for a detailed description of the data-processing steps. The result is global grid (4000×2000 pixels) of brightness temperature data, available by date. The data of the current day are recalculated whenever new swath data are available.

In order to compensate for missing data (in particular around the equator) and to eliminate some noise, a 4-day average is calculated for each pixel, starting with the day of interest and going 4 days back. The 4-day window ensures at least two data points for each pixel.

Flood signals are calculated for each pixel as soon as new data are available (using a local maximum as the calibration temperature), resulting in a 'water signal image' showing standing surface water. Using the statistics of a 7-year time series, the magnitude for each pixel is calculated, too.

Figure 2 describes the systems involved in the flood disaster alert system. There are five independent systems involved. Three systems for flood detection: Jaxa/NASA's AMSR-E system (itself composed of many systems), the Jaxa and/or NSIDC distribution system and the JRC Global Flood Detection System (GFDS). Two systems for flood impact analysis were used: a global spatial data infrastructure (GSDI) with data on population distribution, populated places and infrastructure globally; and the Global Disaster Alert and Coordination System (GDACS), which is a multihazard alert system to which the Global Flood Detection System provides flood alerts for further processing with impact models (De Groeve *et al.* 2010). GDACS combines information on the hazard with information on the exposed population to assess the hazard impact, and has the ability to compose and send alert messages.

On average, the time between the flood event and the flood alert is between 2 and 26 h. Since the satellite passes most locations on earth once per day, the delay between flood (t_0) and observation (t_1) is between 0 and 24 h, with an average of 12 h. From the time of observation to publication on the Jaxa ftp site (t_2) on average 2 h elapse. A download at JRC of one AMSR-E track file takes on average 5 min. Files are available at JRC for processing (t_5) on average 2 h after observation. Processing at JRC is a matter of minutes. Data for over 10 000 monitoring sites are extracted from the data files in less than 10 s and inserted into a database. The flood signal and magnitude are recalculated with the new data, and XML feeds and web pages are published dynamically.
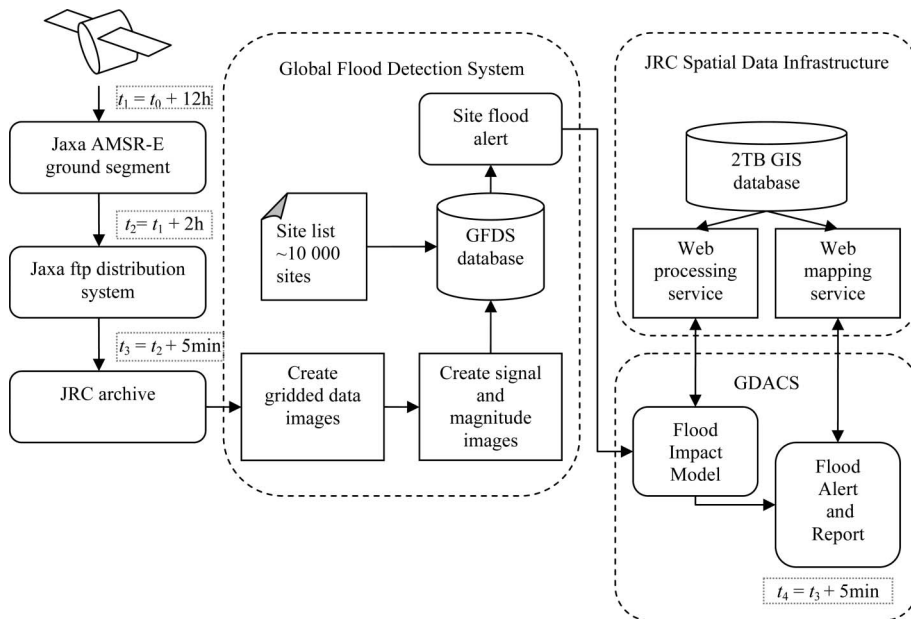

Figure 2.   Overview of systems involved in providing global flood disaster alerts.

2.2   *Flood detection*

For detecting floods, we define a set of monitoring areas for which a virtual hydrograph is calculated. A monitoring area can be a pixel of the grid, or a group of pixels. For each pixel, two measurements are available daily: the water signal s (or M/C ratio) and the magnitude $m = (s - \text{avg}(s))/\text{sd}(s)$. If a monitoring area consists of more than one pixel, we consider the following quantities: average signal, minimum signal, average magnitude, maximum magnitude. In addition, for a monitoring area of more than 1 pixel, we store the number of pixels exceeding magnitude 2 (probability of 2.1%) and the number of pixels exceeding magnitude 4 (probability of 0.003%).

All these quantities are indicative of the size of the flood in the observation area. The average of minimum flood signal is an objective measure of the water surface in the pixel. The average or maximum magnitude is an objective measure of the relative size of the flooding compared for all events since 2002. The pixel count is a measure of the extent of the floods. Since each pixel represents an area of about 100 km^2, the 'number of pixels exceeding magnitude 4' is an approximate measurement of the flooded area (number of pixels × 100 km^2).

We have defined several types of monitoring sites. First, we used 2634 locations defined by the Dartmouth Flood Observatory in locations that previously suffered major floods or that have a high flood risk (Brakenridge *et al.* 2007). The sites are defined by geographical latitude and longitude. We created monitoring areas using the pixel covering that geographical location. Second, we defined 4475 areas as linear segments of 50 km in length on major rivers. Third, we created a web-based application where hydrological services or water authorities can define their own 'virtual gauging sites'. With intimate knowledge of the local river network, they are able to understand where to best locate sites for early flood alerting. In November 2009, 27 sites were set up by the Namibian hydrological service.

In order to detect floods automatically, a set of threshold needs to be defined on one or more quantities, distinguishing between various flow states. We defined three flow states: green (normal or low flow), orange (flood) and red (major flood). We set thresholds at magnitude 2 and 4, respectively, for orange and red floods.

2.3   *Flood mapping*

The term 'flood map' is used for many cartographic products, sometimes leading to confusion with emergency managers. Typically, a flood map should show the maximum extent of a flood event. Since floods often propagate downstream, they are a dynamic phenomenon, and flood maps of different times are necessary to give a complete picture. Satellite-based flood maps are often mapping the flood extent at a given day, not necessarily at the peak of the floods, but rather when a satellite image was acquired. Flood maps should also show the difference with reference water, highlighting the abnormal surface water.

With a resolution of 10 km^2, one can hardly speak of flood extent mapping for the microwave derived products described in this article. At best, the maps indicate areas where floods occur, not the precise extent. It is possible to indicate if the area around a town is flooded, but not if the town is flooded. However, this method provides maps with a high temporal resolution (1 day), which is suitable for mapping the

dynamic aspects of floods, such as the downstream propagation or the growth and recession of flood waters.

To produce flood maps, colour palettes are defined to render the water signal and magnitude values. The water signal is shown in blue shades ranging from dark blue ($s < 0.5 \Leftrightarrow w \approx 100\%$) to white ($s < 0.9 \Leftrightarrow w \approx 0\%$). Pixels with values larger than 0.9 are made transparent. The magnitude is shown in shades ranging from yellow (magnitude 2) to red (magnitude 5 or larger). Magnitudes below 2 are transparent.

Global flood map images are generated automatically as soon as new data arrive. However, flood maps are most meaningful in a temporal and spatial context: around an observation site, around a city of interest, showing a river or showing a regional overview map. In addition, maps should not be created for periods when no flooding occurs. Therefore, in case a flood event occurs, flood maps are generated automatically for each of the defined monitoring sites defined in the previous section. If the magnitude exceeds a threshold, map images are generated for an area expanded 200 km in each direction around the monitoring site from 10 days before to the end of the flood event, and published on the website. In addition, an animation is created for those images, effectively creating a movie showing the daily evolution of the flood. This ensures timely flood map (and animation) creation for monitoring sites.

However, to ensure timely flood maps for other areas, a web-based application was created where emergency managers or hydrological services can interactively create flood maps or animations of an arbitrary area of interest for a given period.

2.4 *Flood size comparison*

A challenge for humanitarian organizations, but also for national governments and reinsurance companies, is to estimate the size of the floods, be it in terms of affected population, damage or cost of reconstruction. There is no single measurement that characterises the strength of the hazard, such as Richter magnitude for earthquakes or Saffir–Simpson categories (based on maximum sustained wind speed) for tropical cyclones. Floods are characterized by their return period, but while this measure is related to the risk of occurrence, it is not related to the affected area.

We will define a measure for flood size based only on the spatial and temporal extent of a flood event, as recorded by passive microwave remote sensing. For the spatial dimension, we use the average flood magnitude for a monitoring site, as defined earlier in the section on flood detection. Since the water signal is proportional to the water content of a pixel (equation (4)), the sum of all pixel values in an area is proportional to the water content of the whole area. The same does not hold for the magnitude, since it is scaled by the standard deviation of each pixel. However, the average magnitude in the area remains an objective measure of the anomaly. To consider the time dimension, the data must be integrated over time. This is achieved by averaging magnitude over time in a time window.

For real-time processing, we consider for each year a window of 30 days back from the current day, and we average the magnitude of the monitoring site. This allows the current flood status to be compared with a similar period in earlier years. For interactive data processing (through a web application or a desktop application), an arbitrary time window can be set. The result is a measure taking into account time and space, and making floods directly comparable across years.

2.5 *Validation*

The methodologies for detection, mapping and sizing of floods were tested in various flood events, but in particular in Namibia for the floods in early 2009. For flood detection, the flood signal and magnitude were compared with hydrograph data from Namibian hydrograph stations, media reports on flood arrivals and situation reports of emergency responders. For flood mapping, the maps were compared with high-resolution satellite flood maps. For flood sizing, the data were compared with information from situation reports and humanitarian funding decisions.

3. Results

3.1 *Flood detection*

The Global Flood Detection System has been producing flood alerts since 2007, with progressively improved methods. Previous validation studies (Kugler and De Groeve 2007, De Groeve and Riva 2009) have shown that, on a global scale, the system can detect floods in some cases up to 10 days before the international media (which is the usual source for information on floods). However, Kugler and De Groeve (2007) showed that omission and commission errors are significant if single pixels are used as observation sites.

   To find the sources for omission and commission errors, we take a closer look at the results in Namibia. Satellite-based flood data match closely in-site hydrograph data. For the station of Katima Mulilo, on the border of Angola and Namibia, where the Zambezi River enters Namibia, we established an observation area. Unfortunately, the area yields rather noisy data (figure 3). Nevertheless, major flood events are clearly identifiably in both systems. For flow rates below 3000 m^3/s, there is no correlation with flood magnitude, because the river stays in the bank. However, for flow rates over 3000 m^3/s, clear peaks are visible in the flood magnitude time series.
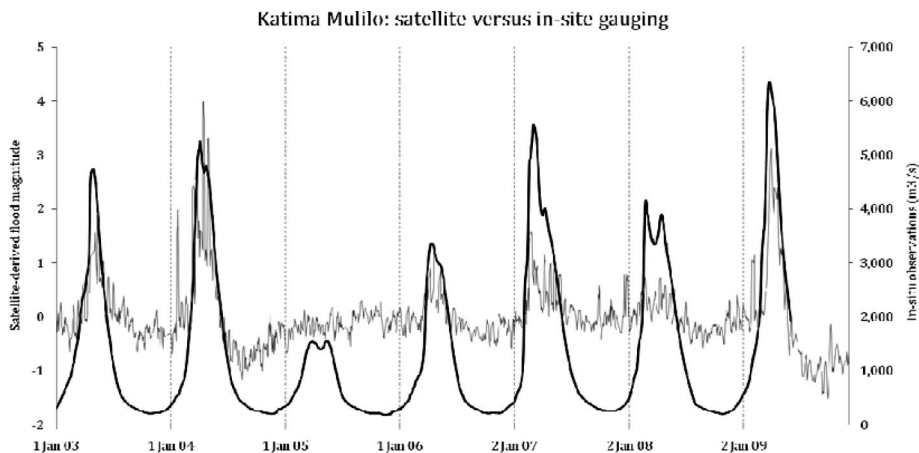

Figure 3. Time series at Katima Mulilo (Namibia). Hydrograph data courtesy of the Namibian Hydrographic Server. For flow rates over 3000 m^3/s, the satellite signal is equivalent.

Other monitoring areas yield less noisy signals, and these can be used for flood detection. For instance, a site on Kalangola (150 km upstream of Katima Mulilo, in Zambia) delivers a very clear signal, which correlates well with the Katima Mulilo *in situ* gauging data (figure 4). To compare the timing of the peaks, we took the date at which the magnitude exceeded 2 (for satellite based gauging) and the date at which the flow rate exceeded 3000 m^3/s (for in situ gauging). In 2007, Kalangola reached magnitude 2 on 2 February, while Katima Mulilo reached 3000 m^3/s on 10 February, giving an 8-day lead in warning.

Because data are available anywhere, one can also consider sites even further upstream to increase the flood warning lead time. For instance, when compared with a monitoring site 500 km upstream on the Upper Zambezi River (near Lungwevungu), a lead time of up to 30 days can be obtained. The magnitude in Lungwevungu exceeded 2 on 8 January 2007, which is 33 days before the flow rate exceeds 3000 m^3/s in Katima Mulilo (figure 5).

Overall, care must be taken with defining monitoring sites. From the experience of hydrologists in Namibia, some sites perform badly for a variety of reasons. When the river is confined and where flow variations result mainly in water-level changes without much expansion of the water area, the satellite-based signal is only noise and the magnitudes (anomalies in the signal) are meaningless. From experience with Namibian water authorities, river segments may do better than points, because they eliminate some of the random variations. Local heavy rains also affect the signal, as does surface water in local pools, which do not add to the river flow by adding to the signal and the apparent flow.

3.2   *Flood mapping*

A unique feature of the AMSR-E based flood system is the regional extent. Daily global coverage allows the creation of regional overview maps, which cannot be created with high-resolution satellite images which have small footprints. For instance, figure 6 shows the flood situation in spring 2009 in southern Africa. Using
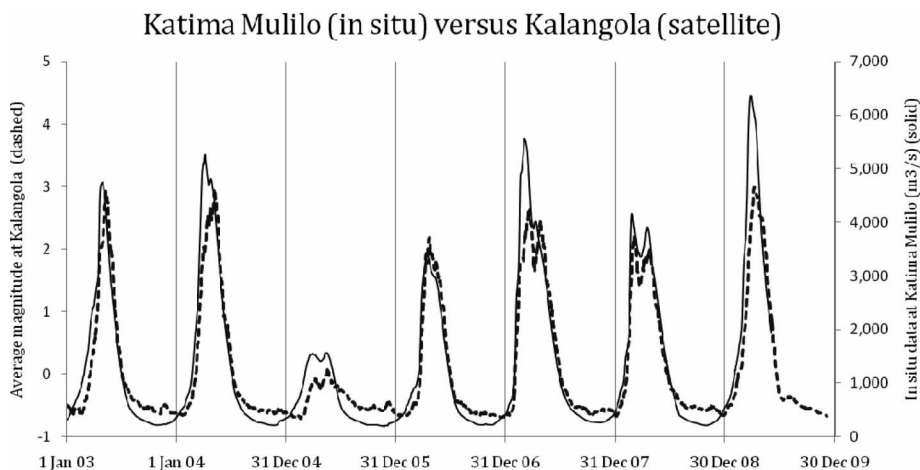

Figure 4.   Flood magnitude at Kalangola (dashed, 12-day moving average) and in situ data at Katima Mulilo (solid).

the water signal (and the blue–white palette described before), the flood areas are clearly visible. In addition, these images are available daily, and the dynamic aspects of floods can be illustrated with animations.

With regards to the accuracy of the maps, we compared the maps in the Caprivi region with high-resolution satellite maps created by UNOSAT (based on various
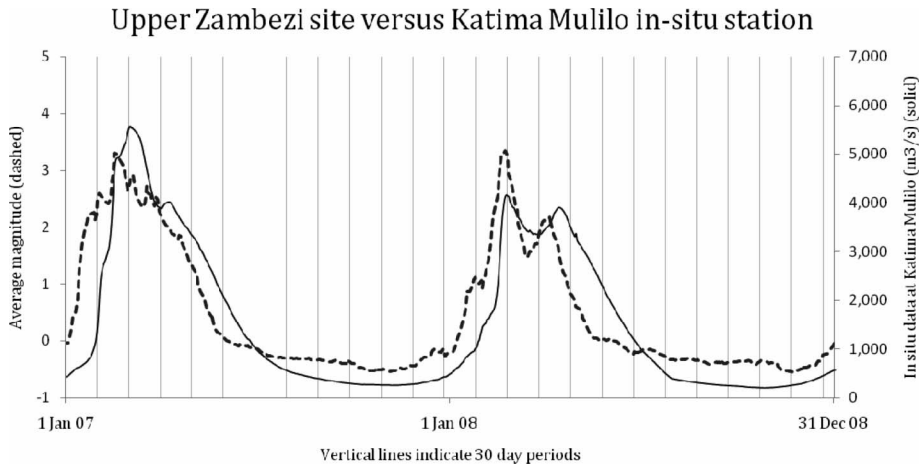

Figure 5.   Flood magnitude at Lungwevungu (dashed, 12-day moving average) and *in situ* data at Katima Mulilo (solid).

Figure 6.   Test areas: floods in Southern Africa, spring 2009 (animation available at http://www.gdacs.org/floods).

high-resolution satellite sensors, including Radarsat, ASAR and DMC data).
Figure 7 shows a map produced by UNOSAT of the Caprivi area, showing the flood
waters on 20 and 29 March in orange and red respectively. Figures 8 and 9 show the
corresponding flood maps created by rendering the water signal of those dates using
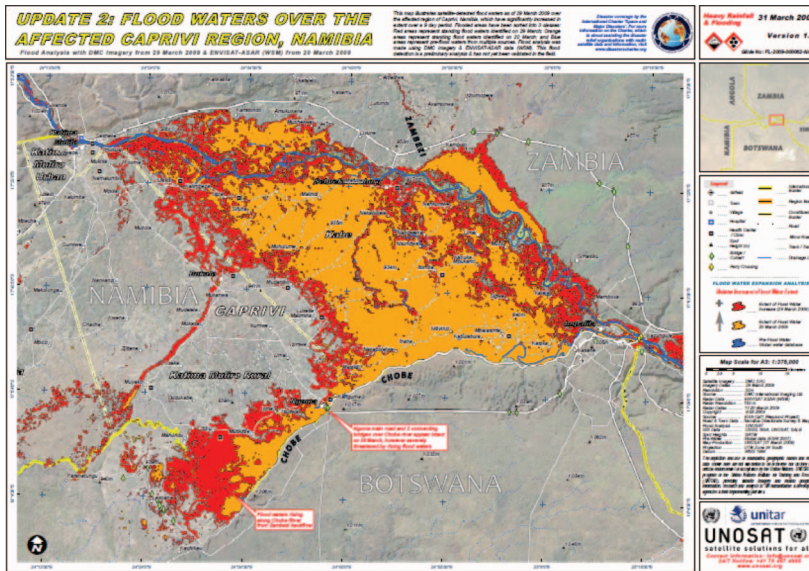

Figure 7.   Flood map, courtesy of UNOSAT, showing the floods on 20 and 29 March 2009.
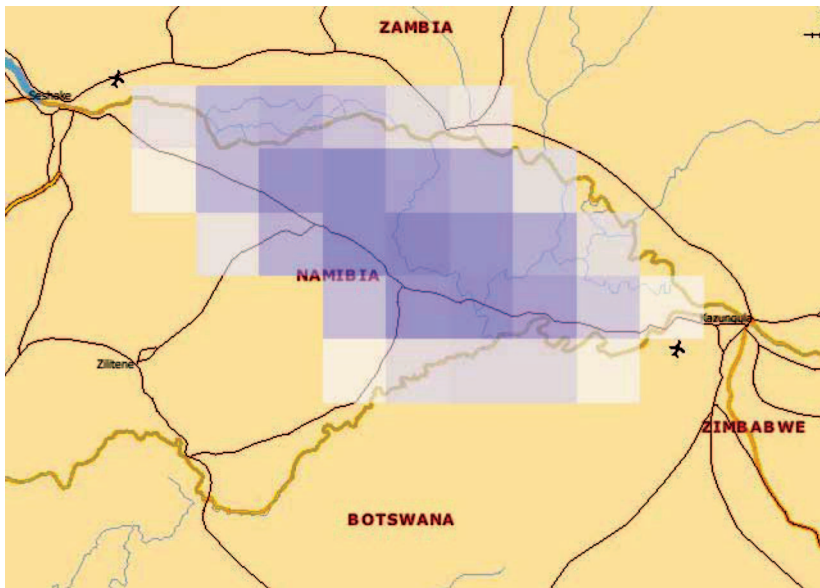

Figure 8.   Flood signal for 20 March 2009, using colour map described in the text, for the
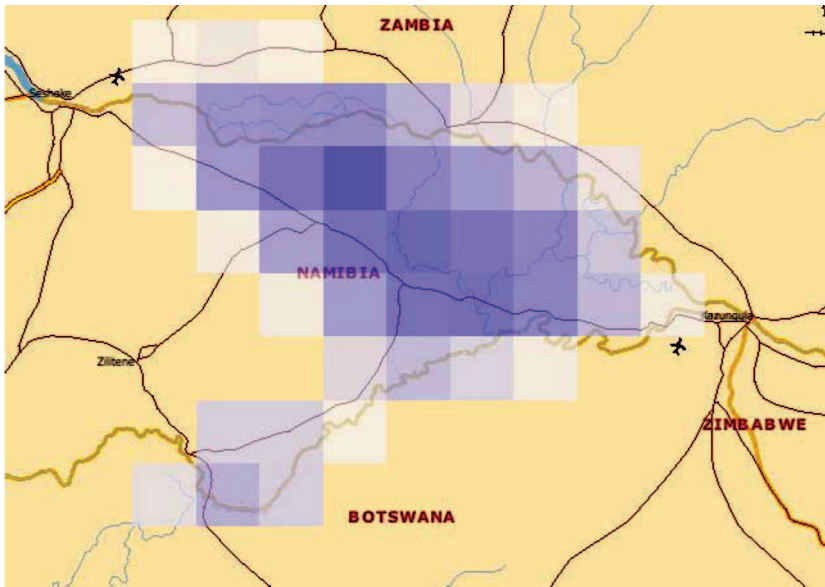same area as figure 7.

Figure 9.   Flood signal for 29 March 2009, using colour map described in the text, for the same area as figure 7.

the colour palette described before. A visual comparison shows a good correspondence between our flood maps and the reference map, with the later floods on the Chobe (to the south-west in the maps) visible only on 29 March.

Because the resolution of the maps is very low, positional accuracy is not a good measure of quality of the maps. However, map quality could be measured quantitatively in terms of the flood extent. Although the flood extent cannot be mapped with such a low resolution, it can be measured because the water signal w is proportional to the surface water extent. The sum $A \sum_A s$ over an area A is a measure for the water surface extent in the area. For 20 and 29 March, we calculated the average water signal s in an area of 110 pixels (covering the floods shown in figures 8 and 9), which was 0.919 and 0.887, respectively (compared with 0.990 for normal flow). If we assume $\varepsilon_{water} = 0.5$ and $\varepsilon_{land} = 1$, then equation (4) can be written as $w = 2(1 - s) \, w = 2(1 - s)$. Applying this formula to the observed values, we estimate 16.2% and 22.6% of land covered by water, compared with a reference value of 2%. Multiplying by the area of observation (110 pixels of approximately 100 km^2), we obtain estimates the flooded area of 1782 km^2 on 20 March 2009 and 2486 km^2 on 29 March 2009, with a reference value of 220 km^2. Since the authors did not have access to the flood polygons of UNOSAT, they redigitized the flood extent and measured a flooded area of 2700 km^2 for 29 March, which is only 8% more than our estimates.

3.3   *Flood sizing*

Many case studies including those described in this paper show that the system is able to provide precise data on starting and ending dates of floods and the size of the floods. While the absolute values of the flood size have not been validated sufficiently against alternative data sources, the relative values are consistent with anecdotal evidence. For instance, for the three areas in southern Africa shown in figure 6, we

Table 1.   Average flooded area (km^2) from February to May (4 months) of each year.

	Border Namibia Angola	Caprivi Region	Upper Zambezi
2009	2000	1330	1330
2008	1360	700	260
2007	300	60	190
2006	280	160	90
2005	80	140	30
2004	60	180	610
2003	120	15	450

calculated the average flooded area over 4 months (from February to May, table 1). The 2008 and 2009 floods stand out clearly, as expected. However, it is also clear that the 2009 floods are worse than the 2008 floods, in particular on the Upper Zambezi. This information is helpful to compare floods objectively with previous floods in order to substantiate humanitarian appeals and funding decisions.

4.   Discussion

Overall, considering the wide range of climate conditions, hydrographic settings, river sizes and flow rates, the technique based on passive microwave remote sensing performs remarkably well. Correlation with hydrograph data has been shown to be excellent. However, sources of noise remain. Under certain conditions, single pixels (or punctual observations sites) will not yield usable data, because the signal-to-noise ratio is close to unity (Kugler and De Groeve 2007). The main reason is related to local conditions on the ground, for instance, if a pixel covers a confined part of a river where flow variations result mainly in water level changes without much expansion of the water area (as was the case for several sites in Namibia).

Combining pixels in larger monitoring areas partially solves this issue. Experience from Namibia shows that larger sites perform better in general (cancelling out sources of noise), but not always. For instance, segments defined in the wrong direction (perpendicular to the river) did not yield an improved signal.

4.1   *Flood detection*

The challenge of automatically detecting floods has not been solved yet. In most cases, magnitude thresholds of 2 (minor flood) or 4 (major flood) yield good results, but not always. Magnitudes are effectively anomalies in a 7-year time series (2002 to now), which is very short compared with return periods of 50 or 100 years of disastrous floods. For many pixels, no major floods occurred in the past 7 years, resulting in low standard deviations. These, in turn, create large magnitudes and therefore many false flood alerts. On the other hand, certain categories of floods cannot be detected, including flash floods (unless the water remain for a few days) and small, local floods. Recent floods in the UK could not be detected conclusively using passive microwave sensing. Although the impact was great, the flooded area was limited to one town district, and much smaller than a pixel of our system.

A solution for false alerts could be to use a cutoff minimum standard deviation in the calculation of the magnitude. This would address cases where no major floods occurred before but would create more flood omissions for small floods like the UK

floods. Alternatively, one could consider the change in magnitude (rather than the value of the magnitude) as a trigger for floods. Typically, magnitudes rise steeply at the onset of floods, resulting in high values for first derivatives. This will be examined in future work.

In practice, the system can be used to detect upstream floods in neighbouring countries. As shown in figure 5, this can result in lead-time warnings of up to 30 days. The use of satellite data can be a cheap alternative for flood early warning without the need for collaboration or approval of the neighbouring governments.

4.2 *Flood mapping*

With regard to mapping, passive microwave sensing can contribute uniquely in two ways: it can provide large overview maps, and it can produce maps on a daily basis. With global coverage and daily temporal resolution, the system provides information that is useful during the response phase. Emergency managers get an overview of the most affected areas, while disaster-mapping organizations can use the overview maps to target high-resolution satellite acquisitions. The high temporal resolution also allows field campaigns to be put into context. Assessment teams visit an affected area during the flood but not necessarily at the peak. Using daily maps, and a satellite hydrograph, it is possible for the assessment team to understand how much worse the situation was before or after the field visit.

The spatial accuracy of the maps could be improved using a digital elevation model. The water content w of a pixel can be derived from the water signal s. If one assumes that the water will be located in the lowest part of the pixel area, a high-resolution digital elevation model can be used to find the lowest portion w of the pixel, which should then be the extent of the flood. This will be addressed in future work.

4.3 *Flood sizing*

The method to estimate the size of a flood event compared with previous years is particularly useful. Because it integrates data over time and space, noise-related or inherent variability of pixel values tends to be cancelled out. The result is a stable and reproducible measure for the size of a flood. The measure is objective and related to the flood extent. However, just as an earthquake's magnitude is not the only factor in an earthquake disaster, the flood magnitude does not consider what has been affected by the water; nor does it take into account water depth. Other data remain necessary to assess the flood impact.

5. Conclusions

This paper shows that global and national flood monitoring can benefit from passive microwave remote sensing. The availability of daily global observations, in combination with a fast data-delivery system and an efficient processing system, allows the fast detection of floods. Quantitative and qualitative measures can be derived to assess the size and extent of the floods. Start and end dates can be objectively determined for any arbitrary place on a river. Extent mapping is only available at a low resolution but at a much higher temporal resolution than other high-resolution satellite maps. It is also the only current solution for flood mapping over large areas (whole countries or continents). In addition, an objective measure of

flood extents can be derived. Applied to the recent floods in southern Africa, the technique allowed a quantitative assessment of the size of the floods relative to previous years to be produced, guiding humanitarian funding decisions and other response decisions. For the 2010 flood season, the system is being fine-tuned in collaboration with the Namibian hydrological authorities and hopefully will provide improved monitoring in the region.

Acknowledgements

References

BJERKLIE, D.M., DINGMAN, S.L., VOROSMARTY, C.J., BOLSTER, C.H. and CONGALTON, R.G., 2003, Evaluating the potential for measuring river discharge from space. *Journal of Hydrology*, **278**, pp. 17–38.

BRAKENRIDGE, G.R., NGHIEM, S.V., ANDERSON, E. and CHIEN, S., 2005, Space-based measurement of river runoff. *Eos*, **86**, pp. 185–188.

BRAKENRIDGE, G.R., NGHIEM, S.V., ANDERSON, E. and MIC, R., 2007, Orbital microwave measurement of river discharge and ice status. *Water Resources Research*. **43**.

DANKO, D.M., 1992, The digital chart of the world project. *Photogrammetric Engineering and Remote Sensing*, **58**, pp. 1125–1128.

DE GROEVE, T., 2007, Global disaster alert and coordination system: more effective and efficient humanitarian response. In *The 14th TIEMS Annual Conference 2007 Book of Proceedings*. Trogir, Croatia (Hydrographic Institute of the Republic of Croatia), pp. 324–334.

DE GROEVE, T., ANNUNZIATO, A., KUGLER, Z. and VERNACCINI, L., 2010, Near real-time global disaster impact analysis. In *Information Systems for Emergency Management*, B. Van De Walle, M. Turoff and S.R. Hiltz (Eds), pp. 302–326 (London: M.E. Sharpe).

DE GROEVE, T., KUGLER, Z. and BRAKENRIDGE, G.R., 2006, Near real time flood alerting for the global disaster alert and coordination system. In *Proceedings ISCRAM2007*, B. Van De Walle, P. Burghardt and C. Nieuwenhuis (Eds), pp. 33–39 (Newark, NJ: ISCRAM).

DE GROEVE, T. and RIVA, P., 2009, Early flood detection and mapping for humanitarian response. In *Proceedings of the 6th International ISCRAM Conference*, J. Landgren, U. Nulden and Bartel Van De Walle (Eds), pp. 1–13 (Gothenburg, Sweden: ISCRAM).

DE GROEVE, T. and RIVA, P., 2009, Global real-time detection of major floods using passive microwave remote sensing. In *Proceedings of the 33rd ISRSE Conference*. Stresa, Italy, pp. 1–4.

DFO, 2009, *Global Active Archive of Large Flood Events*. Available online at: http://www.dartmouth.edu/~floods (accessed 25 February 2009).

FTS OCHA, 2009, *Financial Tracking Service*. Available online at: http://ocha.unog.ch/fts (accessed 25 February 2009).

KUGLER, Z. and DE GROEVE, T., 2007, *The Global Flood Detection System* (Luxembourg: Office for Official Publications of the European Communities).

REES, W.G., 1990, *Physical Principles of Remote Sensing* (Cambridge: Cambridge University Press).

RODRIGUEZ, J., VOS, F., BELOW, R. and GUHA-SAPIR, D., 2009, *Annual Disaster Statistical Review 2008* (Brussels: Centre for Research on the Epidemiology of Disasters).

SMITH, L.C., 1997, Satellite remote sensing of river inundation area, stage and discharge: A review. *Hvdrological Processes*, **11**, pp. 1427–1439.

USGS, 1998, *A New Evaluation of the USGS Streamgaging Network*. *A report to Congress*. Available online at http://water.usgs.gov/streamgaging/report.pdf (accessed 25 Feb 2009).

VAN LANGENHOVE, G., 2009, *Crisis Mapping*. Available online at http://crisismapping.ning.com/xn/detail/3244260:Comment:4477 (accessed 12 June 2009).